Journal of Materials Chemistry

Cite this: *J. Mater. Chem.*, 2011, **21**, 12449

www.rsc.org/materials

PAPER

Ultrahigh density array of CdSe nanorods for CdSe/polymer hybrid solar cells: enhancement in short-circuit current density

Seungchul Kwon,[a] Myungsun Shim,[b] Jeung In Lee,[a] Tae-Woo Lee,*[c] Kilwon Cho[b] and Jin Kon Kim*[a]

Received 6th May 2011, Accepted 7th June 2011
DOI: 10.1039/c1jm11990g

We fabricated CdSe/poly(3-hexylthiophene) (P3HT) hybrid solar cells with ultrahigh density array (4×10^{11} in^{-2}) of the CdSe nanorods having a length of ~100 nm, a diameter of ~20 nm, and an inter-distance of neighboring nanorods of ~20 nm. The vertically oriented CdSe nanorods on indium tin oxide-coated glass were prepared by electrodeposition into a nanoporous template made of polystyrene-*block*-poly(methyl methacrylate) copolymer (PS-*b*-PMMA) thin film. The short-circuit current of this device was three-times greater than that of another solar cell prepared by CdSe/P3HT bilayer film, indicating that more efficient charge separation at the interface and facilitated charge transport were achieved through the vertically oriented CdSe nanorods. The power conversion efficiency of the solar cell based on CdSe nanorod array/P3HT hybrid was twice greater than that of another based on CdSe/P3HT bilayer films.

Introduction

Polymer solar cells fabricated by spin-coating,[1–7] spray-coating,[8–10] and roll-to-roll printing[11] have gained great attention because of simple fabrication and low cost. Recently, organic/inorganic hybrid solar cells[12] have been extensively investigated using poly(3-hexylthiophene) (P3HT) as an organic electron donor material and different kinds and shapes of inorganic semiconductors, for instance CdSe,[13,14] PbS,[15] PbSe,[16] $CuInS_2$,[17] $CuInSe_2$ nanoparticles,[18] CdSe nanorods,[19] CdSe tetrapods,[20] and CdSe hyper-branched shapes,[21] as an electron acceptor. This is because of higher electron mobility of inorganic semiconductor,[22] light absorption, and air stability[23] compared to those of the commonly used phenyl-*C*61-butyric acid methyl ester.

For polymer/inorganic bilayer films, the generated excitons in the donor materials can decay radiatively or nonradiatively during their diffusion to the donor–acceptor (DA) interface where they are separated into holes and electrons. Also, the DA interface area is very small. Hybrid solar cells using inorganic nanostructures, however, could overcome these disadvantages, because they show enhanced short-circuit current density (J_{SC}) and fill factor (FF) compared with those of the bilayer solar cells.[24,25]

On the other hand, for a polymer/inorganic nanoparticle blend system, although the DA interface area is increased, the polymer and inorganic particles often phase-separate in a scale which is much larger than the exciton diffusion length of the electron donor materials upon spin-coating an organic/inorganic hybrid photoactive layer on a substrate.[26,27] If the nanoparticles, however, are non-aggregated using amino-functionalized polymer to avoid phase separation,[12,14,28,29] non-aggregated nanoparticles could not make a pathway of electrons and touch the electrode, which results in many dead points.

The best geometry would be an interdigitated (or ordered) DA heterojunction morphology in the active layer. The interdigitated structures are favorable to increase the exciton dissociation efficiency through large DA interfaces and to facilitate the carrier transport to each electrode without dead ends.[30] For all generated excitons to exist within a diffusion length to the DA interface, a hole-conducting polymer such as P3HT should fill the gap between vertically well-ordered inorganic nanorods on the order of exciton diffusion length of P3HT (~10 nm).[27]

Many nanostructured hybrid solar cells using the inorganic nanostructure have been prepared by chemical vapor deposition,[31] electrodeposition,[32] pulsed current electrolysis method,[33] chemical solution routes,[25,34,35] and sol–gel reaction.[36] However, the distance between two neighboring nanostructures is much larger than the exciton diffusion length.[27] Although the well-ordered nanostructure with the spacing shorter than exciton diffusion length of a donor polymer could be prepared by infiltration into a nanoporous template utilizing the capillary force,[24] the method could not easily produce a large area with a uniform spacing.

We realize that when a nanoporous template based on diblock copolymer is used, the inorganic semiconductor nanostructure with the spacing shorter than exciton diffusion length could be easily achieved over a large area.[37,38] Here, we fabricated

[a]*National Creative Research Center for Block Copolymer Self-Assembly, Pohang University of Science and Technology, Gyeongbuk, 790-784, Korea*
[b]*Department of Chemical Engineering and Polymer Research Institute, Pohang University of Science and Technology, Gyeongbuk, 790-784, Korea*
[c]*Department of Materials Science and Engineering, Pohang University of Science and Technology, Gyeongbuk, 790-784, Korea. E-mail: jkkim@postech.ac.kr; twlee@postech.ac.kr; Fax: +82 279 8298*

a ultrahigh density array of CdSe nanorods having 20 nm in diameter and 20 nm in rod-to-rod spacing onto an indium tin oxide (ITO)-coated glass substrate by electrodeposition of CdSe precursor ($CdSO_4$ and SeO_2) inside a nanoporous template prepared by polystyrene-*block*-polymethylmethacrylate copolymer (PS-*b*-PMMA) thin film.[39–43] The nanopores in the template are hexagonally packed and vertically oriented to the ITO substrate. Since P3HT is filled into the empty spaces between CdSe nanorods, most of excitons generated in the P3HT phase can be diffused to the DA interface and dissociated into holes and electrons without recombination. Furthermore, vertically aligned CdSe nanorods on the ITO could provide a direct charge transport pathway of electrons without dead ends and increase the interface area between P3HT and CdSe for charge dissociation. We found that the solar cells based on CdSe nanorods/P3HT in this study exhibited three times larger J_{SC} and the two-fold power conversion efficiency (PCE) compared with those obtained from a solar cell based on CdSe/P3HT bilayer thin film.

Experimental

Materials

PS-*ran*-PMMA copolymer with hydroxyl end-functional groups (the number average molecular weight (M_n) = 7400, weight fraction of PS (w_{PS}) = 0.596, and polydispersity index (PDI) =1.60) and PMMA homopolymer (M_n = 16 800 and PDI = 1.08) were purchased from Polymer Source Inc. PS-*b*-PMMA (M_n = 75 600, w_{PS} = 0.754, and PDI = 1.21) was synthesized in this lab by atom transfer radical polymerization.[38] Cadmium sulfate ($CdSO_4$, 99.99+%, Aldrich), selenium dioxide (SeO_2, 99.9+%, Sigma-Aldrich), sulfuric acid (H_2SO_4, 97%, Matsunden Chemicals Ltd), methanol (CH_3OH, 99.5%, Samchun Chemicals), phosphoric acid (H_3PO_4, 85%, Samchun Chemicals), 4-aminobenzenethiol ($C_6H_4SHNH_2$, TCI), *o*-dichlorobenzene ($C_6H_4Cl_2$, 99%, Aldrich) were used without further purification. P3HT with regioregularity of 90–93% was purchased from RIEKE Metal Co.

Preparation of nanoporous template

An ITO-coated glass was rinsed by using acetone for 5 min, ethanol for 5 min, 3 wt% Mucasol solution in deionized (DI) water for 20 min and washed again with DI water. Then, it was treated with UV/ozone to modify the surface with hydroxyl groups. The mixture of PS-*b*-PMMA/PMMA homopolymer was spin-coated on ITO modified with a hydroxyl-terminated PS-*ran*-PMMA brush. A nanoporous template was prepared by removing the PMMA block and the PMMA homopolymer using UV irradiation in vacuum and acetic acid which is a selective solvent to PMMA.[38]

Electrodeposition of CdSe

$CdSO_4$ (25.0 mg, 2 mmol) and SeO_2 (1.33 mg, 0.2 mmol) were dissolved in a mixture of DI water (30 ml) and methanol (30 ml) containing H_2SO_4 (40 μl). ITO was used as a working electrode, while Ag/AgCl was used as a reference electrode, and platinum plate as a counter electrode. CdSe was electrochemically deposited inside the nanopores starting from the bottom of the ITO at an applied potential of −0.60 V based on the Ag/AgCl reference electrode by using a PowerLab/4SP potentiostat (AD Instruments). The electrodeposition time was carefully adjusted so that CdSe nanorods were grown only inside the nanoporous template.

Fabrication of solar cells

Fig. 1 shows a schematic of the fabrication of hybrid solar cells based on P3HT and CdSe nanorods. After electrodeposition of CdSe with a length of ~100 nm inside the nanoporous template, the template was completely removed by burning at 500 °C for 40 min in air. We also prepared another solar cell based on P3HT/CdSe bilayer thin film without using the nanoporous template. The CdSe films and nanorod arrays were dipped in ethanol with 5 wt% H_3PO_4 for 60 min to etch any oxidized CdSe surface. Then, they were quickly dipped in ethanol solution with 2 mmol 4-aminobenzenethiol for 6 h to prevent further oxidation at the surface of CdSe. They were washed again with fresh ethanol, and kept in vacuum to remove completely the residual solvent. Next, P3HT in chloroform or in dichlorobenzene (DCB) solutions (20 mg in 1 ml) was spin-coated onto preformed CdSe thin film and nanorod arrays and annealed at 185 °C for 10 min, and cooled slowly. Finally, MoO_3 (15 nm in thickness) and Ag (80 nm) layers were prepared by sequential deposition on the P3HT surfaces. These layers were used as a hole-transporting layer and an anode, respectively, while ITO acted as a cathode.

Characterization

Atomic force microscopy (AFM) (Digital Instrument D3000) in the tapping mode with silicon nitride tips on cantilevers (Nanoprobe) was used to characterize surface morphology of the nanoporous template. Tilted and cross-sectional images were obtained using field emission scanning electron microscopy (FE-SEM) (Hitachi S-4800) operating at 3–10 kV. High resolution transmission electron microscopy (HR-TEM) and energy dispersive X-ray spectroscopy (EDS) (JEOL JEM-2010F) were used to characterize a single CdSe nanorod. For this purpose, the vertically aligned nanorods on the ITO glass were scratched by a single-edged blade and dispersed in ethanol using sonication. The ethanol solution was dropped on the carbon-coated TEM grid and the ethanol was completely removed. The crystal structure of the ultrahigh density array of CdSe nanorods on the ITO glass was characterized with grazing incidence X-ray diffraction (GIXD) experiment with a synchrotron source at

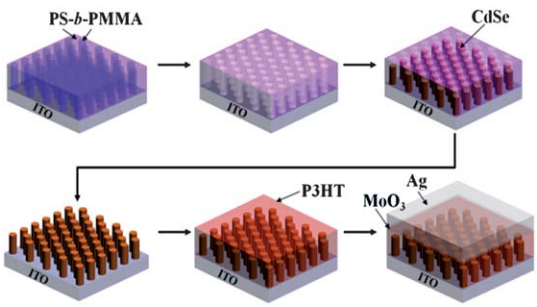

Fig. 1 A schematic for preparation of CdSe nanorods/P3HT hybrid solar cells.

Pohang Accelerator Laboratory (PAL) (beamlines 3C2 and 10C1 of Pohang Light Source) for CdSe nanorod array.

Results and Discussions

Fig. 2(a) shows an AFM phase image of the nanoporous template on the ITO substrate after removing the PMMA phase. Both the pore diameter and the interdistance between two neighboring pores are almost the same (~20 nm). Fig. 2(b) gives a cross-sectional FE-SEM image of as-electrodeposited CdSe nanorods inside the nanoporous template, showing that CdSe nanorods were successfully prepared inside the nanoporous template starting from the ITO substrate. After the nanoporous template was removed, an ultrahigh density array (4×10^{11} in^{-2}) of vertically aligned CdSe nanorods was achieved on the ITO substrate. Fig. 2(c) shows a 65° tilted FE-SEM image of the CdSe nanorod arrays. The vertical orientation of the CdSe nanorods on the ITO substrate was maintained, even if the template was removed by thermal combustion at 500 °C. Fig. 2(d) shows a cross-sectional FE-SEM image of the ultrahigh density array of vertically aligned CdSe nanorods on ITO substrate.

Fig. 3(a) shows a TEM image of a single CdSe nanorod. The diameter of the CdSe nanorod was ~20 nm, which is the same as that of the pores in the template. Fig. 3(b) shows a selected area electron diffraction (SAED) pattern of the CdSe nanorod, indicating that the CdSe nanorod has a wurtzite crystal structure. The distinct (002) spot suggests that the CdSe nanorod preferably grew along the (002) direction. This might be due to the cylindrical confinement in a nanoscale (~20 nm) and annealing at high temperature of 500 °C. The interplanar distance of the [001] crystal face was obtained as 0.347 nm (Fig. 3(c)). Fig. 3(d) shows the EDS spectrum of CdSe nanorods, showing equal elemental composition of cadmium and selenium in a CdSe nanorod.

The crystal structure of CdSe nanorods vertically aligned on the ITO substrate was measured by GIXD experiments. Fig. 4 shows a $\theta-2\theta$ scan along the normal direction to the substrate, from which the CdSe (002) peak was clearly observed at 25.4°. Based on HR-TEM and GIXD results, we can conclude that the vertically aligned CdSe nanorods exhibited hexagonal wurtzite crystal structure in the large area, and the growth direction of CdSe nanorods was [001] direction.

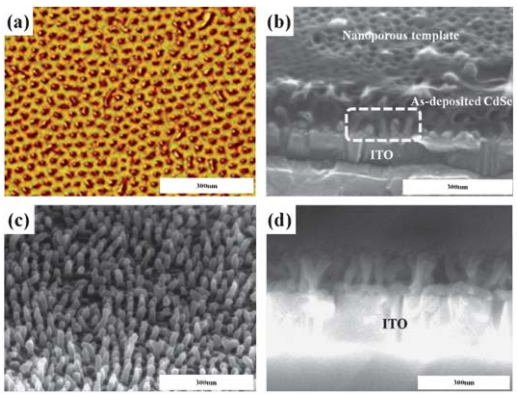

Fig. 2 (a) AFM phase image of nanoporous template, and FE-SEM images of (b) cross-sectional view of as-deposited CdSe in the nanoporous template, (c) 60° tilted image, and (d) cross-sectional views of CdSe nanorods after removing the nanoporous template.

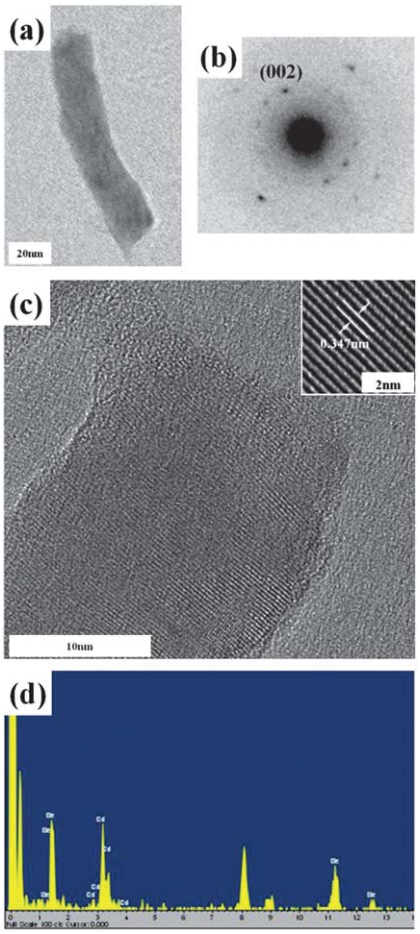

Fig. 3 (a) A TEM image, (b) SAED pattern, (c) HR-TEM image, and (d) EDS spectrum of a single CdSe nanorod.

Fig. 5(a) and (b) shows the cross-sectional FE-SEM images of spin-coated P3HT layers on the CdSe nanorod arrays, followed by annealing at 185 °C for 10 min. When the P3HT layer was spin-coated from chloroform solution, P3HT did not fill completely the interspace of CdSe nanorods, and many voids

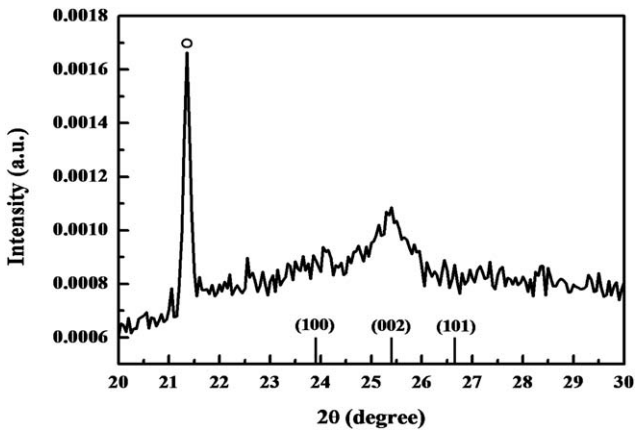

Fig. 4 $\theta-2\theta$ scan of CdSe nanorod array on ITO. The diffraction peak of the ITO substrate is marked by a circle.

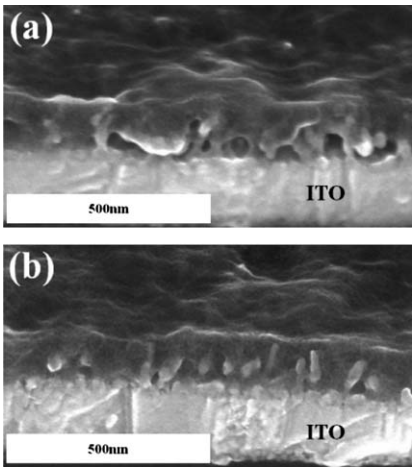

Fig. 5 Cross-sectional FE-SEM images of the CdSe nanorod array/P3HT spin-coated from (a) chloroform and (b) DCB followed by annealing at 185 °C.

were observed (Fig. 5(a)). On the other hand, when P3HT was spin-coated from DCB solution, the interspace of CdSe nanorods was completely filled with P3HT (Fig. 5(b)). Different coverage of P3HT between the nanorods might be attributed to the different boiling points of the solvents.[44]

Fig. 6(a) gives the current density–voltage (J–V) characteristics of solar cells measured under the solar-simulated air mass (AM) 1.5 G illumination at an intensity of 100 mW cm^{-2} for a CdSe/P3HT bilayer film and a CdSe nanorod array/P3HT. The J_{SC} of a solar cell based on the CdSe nanorod array was 3.20 mA cm^{-2}, which was three times larger than that (1.08 mA cm^{-2}) of another solar cell prepared from the CdSe/P3HT bilayer thin film. Also, the fill factor (FF) was slightly increased from 0.34 to 0.38. The power conversion efficiency (PCE) of the former cell was 0.28%, which is ~2.15 times larger than that (0.13%) of the latter cell. It is noted that the optical absorbances in UV/Vis wavelengths of CdSe film and nanorod array are almost identical (data are not shown here). Thus, the enhancement in the J_{SC} for the CdSe nanorods array comes mainly from the increased interface area (~4 times) between P3HT and CdSe nanorods. Considering the areal density of 4×10^{11} in^{-2} and the height of 100 nm of CdSe nanorods, the surface area of CdSe nanorod arrays was 4 cm^2 on 1 cm^2 ITO.

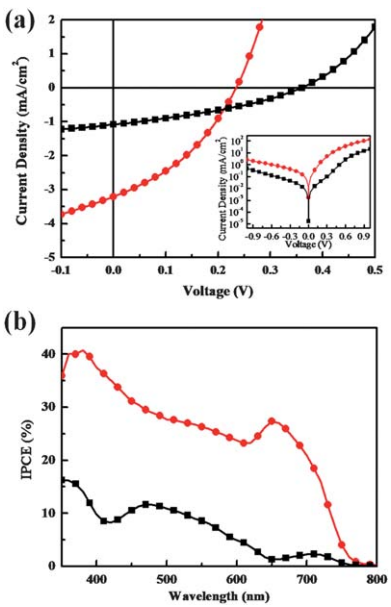

Fig. 6 (a) The J–V characteristics measured under the illumination of AM 1.5 G full sunlight (100 mW cm^{-2}). The inset is corresponding to dark current measurement, and (b) incident photon-to-current conversion efficiency (IPCE) spectra of CdSe film/P3HT solar cell (■) and CdSe nanorod array/P3HT solar cell (●).

Fig. 6(b) shows the incident photon-to-current efficiency (IPCE) spectra of solar cells based on CdSe nanorod array and bilayer film. For the bilayer geometry, the IPCEs were below 15% in the wavelength from 350 nm to 800 nm. However, the solar cell based on CdSe nanorod array was much enhanced (3 times higher). This result again suggests that the larger surface area of CdSe nanorod array mainly contributed to the increase of J_{SC}. The preferred orientation of the CdSe lattice along the nanorods facilitated electron transport, which results in a slight increase in FF. The V_{OC}, however, was decreased from 0.36 to 0.23 V. This might be attributed to the direct contact of P3HT to the ITO cathode in the CdSe nanorod array/P3HT devices, which could reduce built-in-voltage by forming ITO/P3HT/MoO_3/Ag structure. The increased dark current (the inset of Fig. 6(a)) and decreased shunt resistance (from 11.5 kΩ in the solar cell based on CdS/P3HT bilayer to 3.1 kΩ in another solar cell based on CdSe nanorod array/P3HT) could reduce the V_{OC}.[45–47] We expect that V_{OC} and FF would be further increased by the introduction of a proper buffer layer such as ZnO and TiO_2 between ITO and the CdSe nanorod array/P3HT active layer,[48,49] which would be a future research subject.

Conclusions

In summary, we fabricated ultrahigh density array (4×10^{11} in^{-2}) CdSe nanorod arrays vertically oriented to ITO substrate using nanoporous block copolymer template. The crystal growth of the nanorods is in the (002) direction. The J_{SC} of a solar cell based on CdSe nanorods/P3HT was three times greater than that of another solar cell based on CdSe/P3HT bilayer thin film. This is mainly due to the increased interface as well as facilitated charge transport through the vertically oriented CdSe nanorods. The power conversion efficiency of the CdSe nanorod array/P3HT hybrid solar cell was twice greater than that of another solar cell based on the bilayer thin film type of CdSe/P3HT solar cell.

Acknowledgements

This work was supported by the National Creative Research Initiative program of National Research Foundation of Korea (NRF) and NRF Grant (NRF-2009-C1AAA001-0093524) funded by the Korean Government (MEST) . XRD experiment was performed at PLS beamlines 3C2 and 10C1 supported by POSCO and NRF.

Notes and references

1 G. Yu, J. Gao, J. C. Hummelen, F. Wudl and A. J. Heeger, *Science*, 1995, **270**, 1789.
2 G. Li, V. Shrotriya, J. Huang, Y. Yao, T. Moriarty, K. Emery and Y. Yang, *Nat. Mater.*, 2005, **4**, 864.

3 R. Steim, F. R. Kogler and C. J. Brabec, *J. Mater. Chem.*, 2010, **20**, 2499.
4 M. Helgesen, R. Søndergaard and F. C. Krebs, *J. Mater. Chem.*, 2010, **20**, 36.
5 C. J. Brabec, S. Gowrisanker, J. J. M. Halls, D. Laird, S. Jia and S. P. Williams, *Adv. Mater.*, 2010, **22**, 3839.
6 J. H. Park, T.-W. Lee, B.-D. Chin, D. H. Wang and O. O. Park, *Macromol. Rapid Commun.*, 2010, **31**, 2095.
7 T.-W. Lee, K.-G. Lim and D.-H. Kim, *Electron. Mater. Lett.*, 2010, **6**, 41.
8 K. X. Steirer, M. O. Reese, B. Rupert, N. Kopidakis, D. C. Olson, R. T. Collins and D. S. Ginley, *Sol. Energy Mater. Sol. Cells*, 2009, **93**, 447.
9 L.-M. Chen, Z. Hong, W. L. Kwan, C.-H. Lu, Y.-F. Lai, B. Lei, C.-P. Liu and Y. Yang, *ACS Nano*, 2010, **4**, 4744.
10 S.-I. Na, B.-K. Yu, S.-S. Kim, D. Vak, T.-S. Kim, J.-S. Yeo and D.-Y. Kim, *Sol. Energy Mater. Sol. Cells*, 2010, **94**, 1333.
11 F. C. Krebs, *Sol. Energy Mater. Sol. Cells*, 2009, **93**, 465.
12 E. Holder, N. Tessler and A. L. Rogach, *J. Mater. Chem.*, 2008, **18**, 1064.
13 J. D. Olson, G. P. Gray and S. A. Carter, *Sol. Energy Mater. Sol. Cells*, 2009, **93**, 519.
14 I. Kanelidis, A. Vaneski, D. Lenkeit, S. Pelz, V. Elsner, R. M. Stewart, J. Rodíguez-Fernández, A. A. Lutich, A. S. Susha, R. Theissmann, S. Adamczyk, A. R. Rogach and E. Holder, *J. Mater. Chem.*, 2011, **21**, 2656.
15 R. Plass, S. Pelet, J. Krueger and M. Gra1tzel, *J. Phys. Chem. B*, 2002, **106**, 7578.
16 K. S. Leschkies, T. J. Beatty, M. S. Kang, D. J. Norris and E. S. Aydil, *ACS Nano*, 2009, **3**, 3638.
17 W. Yue, S. Han, R. Peng, W. Shen, H. Geng, F. Wu, S. Tao and M. Wang, *J. Mater. Chem.*, 2010, **20**, 7570.
18 E. Arici, H. Hoppe, F. Schaffler, D. Meissner, M. A. Malik and N. S. Sariciftci, *Thin Solid Films*, 2004, **451–452**, 612.
19 W. U. Huynh, J. J. Dittmer and A. P. Alivisatos, *Science*, 2002, **295**, 2425.
20 I. Gur, N. A. Fromer and A. P. Alivisatos, *J. Phys. Chem. B*, 2006, **110**, 25543.
21 I. Gur, N. A. Fromer, C.-P. Chen, A. G. Kanaras and A. P. Alivisatos, *Nano Lett.*, 2007, **7**, 409.
22 J. S. Jie, W. J. Zhang, Y. Jiang and S. T. Lee, *Appl. Phys. Lett.*, 2006, **89**, 133118.
23 I. Gur, N. A. Fromer, M. L. Geier and A. P. Alivisatos, *Science*, 2005, **310**, 462.
24 S. S. Williams, M. J. Hampton, V. Gowrishankar, I.-K. Ding, J. L. Templeton, E. T. Samulski, J. M. DeSimone and M. D. McGehee, *Chem. Mater.*, 2008, **20**, 5229.
25 L. E. Greene, M. Law, B. D. Yuhas and P. Yang, *J. Phys. Chem. C*, 2007, **111**, 18451.
26 S. D. Oosterhout, M. M. Wienk, S. S. van Bavel, R. Thiedmann, L. J. A. Koster, J. Gilot, J. Loos, V. Schmidt and R. A. J. Janssen, *Nat. Mater.*, 2009, **8**, 818.
27 P. E. Shaw, A. Ruseckas and I. D. Samuel, *Adv. Mater.*, 2008, **20**, 3516.
28 I. Kanelidis, V. Elsner, M. Bötzer, M. Butz, V. Lesnyak, A. Eychmüller and E. Holder, *Polymer*, 2010, **51**, 5669.
29 I. Kanelidis, Y. Ren, V. Lesnyak, J.-C. Gasse, R. Frahm, A. Eychmüller and E. Holder, *J. Polym. Sci., Part A: Polym. Chem.*, 2011, **49**, 392.
30 K. M. Coakley and M. D. McGehee, *Chem. Mater.*, 2004, **16**, 4533.
31 C. Xu, K. Yang, L. Huang and H. Wang, *J. Renewable Sustainable Energy*, 2010, **2**, 053101.
32 M. Wang and X. Wang, *Sol. Energy Mater. Sol. Cells*, 2008, **92**, 357.
33 Y.-Y. Lin, C.-W. Chen, T.-H. Chu, W.-F. Su, C.-C. Lin, C.-H. Ku, J.-J. Wu and C.-H. Chen, *J. Mater. Chem.*, 2007, **17**, 4571.
34 A. M. Peiró, P. Ravirajan, K. Govender, D. S. Boyle, P. O'Brien, D. D. C. Bradley, J. Nelson and J. R. Durrant, *J. Mater. Chem.*, 2006, **16**, 2088.
35 P. Ravirajan, A. M. Peiró, M. K. Nazeeruddin, M. Graetzel, D. D. C. Bradley, J. R. Durrant and J. Nelson, *J. Phys. Chem. B*, 2006, **110**, 7635.
36 Q. Wei, K. Hirota, K. Tajima and K. Hashimoto, *Chem. Mater.*, 2006, **18**, 5080.
37 P. Mansky, Y. Liu, E. Huang, T. P. Russell and C. Hawker, *Science*, 1997, **275**, 1458.
38 U. Jeong, D. Y. Ryu, D. H. Kho, J. K. Kim, J. T. Goldbach, D. H. Kim and T. P. Russell, *Adv. Mater.*, 2004, **16**, 533.
39 J. K. Kim, J. I. Lee and D. H. Lee, *Macromol. Res.*, 2008, **16**, 267.
40 J. K. Kim, S. Y. Yang, Y. Lee and Y. Kim, *Prog. Polym. Sci.*, 2010, **35**, 1325.
41 S. Y. Yang, I. Ryu, H. Y. Kim, J. K. Kim, S. K. Jang and T. P. Russell, *Adv. Mater.*, 2006, **18**, 709.
42 W. Joo, M. S. Park and J. K. Kim, *Langmuir*, 2006, **22**, 7960.
43 J. I. Lee, S. H. Cho, S.-M. Park, J. K. Kim, J. K. Kim, J.-W. Yu, Y. C. Kim and T. P. Russell, *Nano Lett.*, 2008, **8**, 2315.
44 H. Bi and R. R. LaPierre, *Nanotechnology*, 2009, **20**, 465205.
45 C. He, C. Zhong, H. Wu, R. Yang, W. Yang, F. Huang, G. C. Bazan and Y. Cao, *J. Mater. Chem.*, 2010, **20**, 2617.
46 A. Molton and J.-M. Nunzi, *Polym. Int.*, 2006, **55**, 583.
47 G. Wei, R. R. Lunt, K. Sun, S. Wang, M. E. Thompson and S. R. Forrest, *Nano Lett.*, 2010, **10**, 3555.
48 J.-P. Liu, K.-L. Choy and X.-H. Hou, *J. Mater. Chem.*, 2011, **21**, 1966.
49 J. Y. Kim, S. H. Kim, H.-H. Lee, K. Lee, W. Ma, X. Gong and A. J. Heeger, *Adv. Mater.*, 2006, **18**, 572.